Available online at www.sciencedirect.com
ScienceDirect
Journal of the European Ceramic Society 31 (2011) 249–257
www.elsevier.com/locate/jeurceramsoc

Ta_2O_5–Y_2O_3–ZrO_2 system: Experimental study and preliminary thermodynamic description

Anup K. Bhattacharya [a,*], Valery Shklover [a], Walter Steurer [a], Gregoire Witz [b], Hans-peter Bossmann [b], Olga Fabrichnaya [c]

[a] *Department of Materials, ETH Zürich, 8093 Zürich, Switzerland*
[b] *ALSTOM (Switzerland) Ltd., 5401 Baden, Switzerland*
[c] *Institute of Material Sciences, Freiberg Mining Academy, 09599 Freiberg, Germany*

Received 16 June 2010; received in revised form 30 August 2010; accepted 6 September 2010
Available online 16 October 2010

Abstract

Some aspects of stable and equilibrium phases in the Ta_2O_5–Y_2O_3–ZrO_2 system have been studied in this work. Phase stability of $Ta_{0.16}Y_{0.16}Zr_{0.68}O_2$ and $Ta_{0.10}Y_{0.10}Zr_{0.80}O_2$ has been studied by X-ray powder diffraction. A secondary phase segregation of $YTaO_4$ has been observed in both compositions below 1500 °C. However, once treated at 1500 °C, $YTaO_4$ phase disappears. The preliminary phase diagram of the Ta_2O_5–Y_2O_3–ZrO_2 system at 1200 °C and 1500 °C have been constructed using THERMOCALC package. Thermodynamic description is obtained by critically evaluating experimental data on the binary systems Y_2O_3–Ta_2O_5 and Ta_2O_5–ZrO_2. Binary system data have been combined and parameters for ternary tetragonal and cubic structures have been assessed to construct ternary phase diagram. Calculated isothermal section at 1200 °C is similar to 1500 °C. There is no change in the tetragonal solid solution region observed with temperature, which indicates the same equilibrium phases at 1500 °C and at 1200 °C.

Keywords: X-ray methods; ZrO_2; Thermal barrier coatings; Phase diagram; Engine component

1. Introduction

New generation of high-efficient gas turbines require new high-temperature stable thermal barrier coating (TBC) materials, which could outperform currently broadly used partially stabilized zirconia (7YSZ, 7–8 wt% Y_2O_3 in ZrO_2). 7YSZ has historically offered the best balance of mechanical and thermal properties needed for gas turbine application. However, 7YSZ formed, for example, under plasma spray conditions consists of predominantly metastable 'non-transformable' t′ phase at room temperature, and undergoes transformation into transformable Y-deficient tetragonal 't' and Y-rich cubic 'c' (fluorite) phases when treated for longer time at and above ~1200 °C: t′ → t + c.[1–3] The transformable t-phase of 7YSZ undergoes martensitic transformation to monoclinic phase (t → m) upon cooling accompanied with detrimental volume expansion (~4–5%). In the search for new TBC suitable for use above 1200 °C, many researchers have tried further doping the YSZ system, for example, with bigger or smaller cations of rare-earth elements.[1,3] Ta-doped YSZ, which is stable up to 1500 °C has been reported as one prospective TBC.[4] The peculiarity of the ZrO_2–$YO_{1.5}$–$TaO_{2.5}$ system is in strong interaction of Y^{3+} and Ta^{5+} cations in tetragonal ZrO_2 matrix, leading to much higher solubility of resulted $YTaO_4$ species compared to the individual solubility of $YO_{1.5}$ and $TaO_{2.5}$.[4–6] The transformability of tetragonal ZrO_2 can be correlated with tetragonality (*c*/*a* ratio), often used for characterization of YSZ and related systems. This correlation was suggested for classification of oxides into stabilizers (decreasing tetragonality) and destabilizers of t-ZrO_2 (increasing tetragonality).[7]

Alloying with Ta_2O_5 decreases stability of both t- and c-phases in the binary ZrO_2–Y_2O_3 system.[5,7] This destabilization can be explained by the increase of the lattice distortions due to alloying with Ta_2O_5 (or with other oxides, for example Nb_2O_5 or HfO_2). On the other hand, incorporation of stabilizing oxides such as Y_2O_3 decreases the tetragonal distortion and increases

* Corresponding author.
E-mail address: anup.bhattacharya@mat.ethz.ch (A.K. Bhattacharya).

0955-2219/$ – see front matter © 2010 Elsevier Ltd. All rights reserved.
doi:10.1016/j.jeurceramsoc.2010.09.009

the stability of ZrO_2 lattice. Stability of ZrO_2 with Y_2O_3 addition was also related to the formation of oxygen vacancies.[8]

However, doping $YTaO_4$ into ZrO_2 increases both its tetragonality and stability. Increased stability in this case was explained by defect association of the smaller Ta^{5+} and bigger Y^{3+} cations in the ZrO_2 lattice.[5] It was shown that 20 mol% $YTaO_4$-stabilized ZrO_2 has a Young's modulus of 150 GPa compared to 200 GPa of 7YSZ. Such a lower modulus and possibility of high coefficient of thermal expansion (CTE) is potential indicator of this system as TBC.

Along with the remarkable phase stability, the $YTaO_4$-doped ZrO_2 system was also found to be suitable for plasma spraying.[9] Strong interaction between Y^{3+} and Ta^{5+} is beneficial for the TBC applications because it (a) leads to remarkably low thermal conductivity even in absence of oxygen vacancies and (b) could reduce individual activities of cations and hence making Y^{3+} cations less susceptible to reaction with foreign ions such as V^{5+}. It has been reported that $YTaZrO_2$ system has higher corrosion resistance against sulfate and vanadate melts as compared to 7YSZ.

It was proposed that 16 mol% $YTaO_4$ doped ZrO_2 is the best TBC candidate as it has the same stability as 20 mol% $YTaO_4$ doped zirconia along with sufficiently low thermal conductivity of 2 W/mK and a fracture toughness of 4 $MPam^{1/2}$, which is twice that of 7YSZ. Besides, 16 mol% $YTaO_4$ doped ZrO_2 has also shown promise in preliminary burner rig test.[9]

Previous works report the presence of single stable tetragonal solid solution of $YTaO_4$–ZrO_2 only at and above 1500 °C.[5] However, presence of $YTaO_4$ phase below 1500 °C was also reported in some other work.[4] Interestingly, once a single tetragonal solid solution is formed at 1500 °C, it becomes stable and thereafter $YTaO_4$ phase separation is not observed even at temperature below 1500 °C.[4] From these observations it may be concluded that single phase tetragonal TaYSZ achieves stability only at 1500 °C and the equilibrium phases below 1500 °C are still unknown.

In order to investigate the low temperature (1200 °C) equilibrium phases in TaYSZ system, we studied ZrO_2 doped with ~20 mol% $YTaO_4$ doped ZrO_2 ($Y_{0.166}Ta_{0.166}Zr_{0.668}O_2$) and ~11 mol% $YTaO_4$ doped ZrO_2 ($Y_{0.1}Ta_{0.1}Zr_{0.8}O_2$). Short-time and long-time stability of these systems at 1250 °C have been studied. Previous data about the ZrO_2–Ta_2O_5–Y_2O_3 system and constituent binaries have been reviewed, phases have been modelled by compound energy formalism and a ternary phase diagram has been calculated using Thermo-calc package.[10,11]

2. Experimental

Starting powders corresponding to $Y_{0.166}Ta_{0.166}Zr_{0.668}O_2$ and $Y_{0.1}Ta_{0.1}Zr_{0.8}O_2$ stoichiometries were prepared by reverse co-precipitation technique. Here onward, these two compositions will be named as 20TaYSZ and 11TaYSZ, respectively. $ZrOCl_2{\cdot}8H_2O$ (99.9%, Alfa-Aesar GmbH, Karlsruhe, Germany), $Y(NO_3)_3{\cdot}6H_2O$ (99.9%, Alfa-Aesar GmbH, Karlsruhe, Germany) and $TaCl_5$ (99.99%, Sigma–Aldrich GmbH, Steinheim, Germany) were used as precursors for precipitation of corresponding hydroxides of Zr, Y and Ta, respectively. Precursors were mixed in ethanol solution and slowly dropped into ammonia solution at pH 10. Precipitates were washed thoroughly, dried overnight and calcined at 1000 °C for 4 h. Calcined powders were annealed at temperatures from 1100 °C to 1500 °C for 4 h. Long-term annealing of the powders was done at 1250 °C for 600 h. For all the heat treatments, heating and cooling rate were maintained at 10 K/min. Phases formed at different temperatures were analysed using X-ray powder diffractometer (Xpert Pro PANalytical, 7600 AA ALMELO, The Netherlands).

3. Thermodynamic assessment of the ZrO_2–Y_2O_3–Ta_2O_5 system

The experimental thermodynamic data and CALPHAD type assessment are not available for ternary ZrO_2–Y_2O_3–Ta_2O_5 system as well as for two constituent binary systems ZrO_2–Ta_2O_5, Y_2O_3–Ta_2O_5 so far. A brief review of all the experimental studies in the binaries and ternaries of this system has been summarised below:

ZrO_2–Ta_2O_5: Only very scarce data are available for phase relations in the ZrO_2–Ta_2O_5 system. Study of Ta_2O_5 rich compositions (5–25 mol% ZrO_2) obtained by solid-state method and heat treated at 1325 and 1410 °C was performed followed by XRD phase identification.[12] At presented schematic diagram, the solubility of ZrO_2 extended up to 10 mol% in the high temperature modification of Ta_2O_5. Several phases with Ta_2O_5/ZrO_2 ratio equal to 6:1, 3:1, 59:6, 27:2, 19:1 and 49:2 were assumed to be stable in the system. A stable orthorhombic phase at Ta_2O_5 concentration of 14.3 mol% was also reported.[13] Extension of homogeneity range of orthorhombic phase was found to be up to ~33 mol% of Ta_2O_5 in ZrO_2. Later on the stability of orthorhombic phase $Ta_2Zr_6O_{17}$ with less extensive homogeneity range between 11 and 17 mol% Ta_2O_5 was confirmed as well as maximum solubility of Ta_2O_5 in ZrO_2 at 2 mol%.[14]

Y_2O_3–Ta_2O_5: Three stable compounds: Y_3TaO_7 with pyrochlore structure having homogeneity range from 20 to 30 mol% of Ta_2O_5, $YTaO_4$ with monoclinic to tetragonal transformation at ~1400 °C and YTa_3O_9 with perovskite structure were found as a result of phase equilibria studies in the Y_2O_3–Ta_2O_5 system.[15] All three compounds melt congruently at 2300, 2060 and 1800 °C, respectively. Four eutectic reactions at 2250, 2000, 1700 and 1750 °C were found.[15]

Investigation of samples obtained by co-precipitation and heat treated at 1250 and 1590 °C has shown that less than 1 mol% of Y_2O_3 is dissolved in the Ta_2O_5 and up to 5% Ta_2O_5 can be dissolved in the Y_2O_3.[16] Several intermediate compounds were found: YTa_7O_{19} with tetragonal structure stable up to 1650 °C, YTa_3O_9 with perovskite structure, $YTaO_4$ with two modifications: monoclinic (low temperature) and tetragonal scheelite type (high temperature) and Y_3TaO_7 with fluorite structure. A new phase, YTa_7O_{19} was found and crystal structure of Y_3TaO_7 phase as fluorite was determined, which was later confirmed by other investigators.[15,17,18] Phase relations in the Y_2O_3–Ta_2O_5 system were also studied experimentally by identification of solid-state reaction products with XRD at 1350–1700 °C and liquidus determination by DTA (differential

thermal analysis).[17,18] Two orthorhombic phases 'O' (30 mol% Ta_2O_5) and 'W2' (25 mol% Ta_2O_5) were found stable at temperatures up to 1900 and 1600 °C, respectively. The fluorite structure (~20 mol% Ta_2O_5) was found stable at temperature above 1550 °C up to congruent melting (2454 °C). Two eutectic reactions were found: (1) at 2220 °C and 8 mol% of Ta_2O_5 and (2) at 1990 °C and 38 mol% Ta_2O_5. It should be mentioned that temperatures of two eutectic reactions and melting temperature of $YTaO_4$ are in a good agreement with that reported elsewhere,[15] while the melting temperature of fluorite structure is ~150 K higher than what was reported before (2300 °C).[15] The fluorite and two orthorhombic phases were not distinguished in previous work on Y_2O_3–Ta_2O_5 system[15] and were presented as series of solid solutions with pyrochlore structure. Two Y_2O_3–xTa_2O_5 compounds with $x = 30$ and 21.5 mol% were synthesised by solid-state reaction at 1700 °C, which possess, according to neutron diffraction, orthorhombic and fluorite structures, respectively.[19] Fluorite type phase with 20 mol% of Ta_2O_5 was also obtained earlier.[20]

ZrO_2–Y_2O_3: One of the authors performed CALPHAD assessment of thermodynamic parameters for the ZrO_2–Y_2O_3 system earlier and presented review of available experimental data (both phase equilibrium data and thermodynamic measurements).[21–23]

ZrO_2–Y_2O_3–Ta_2O_5: Phases in the ZrO_2–Ta_2O_5–Y_2O_3, obtained by co-precipitation and heat treated at 1500 °C,[5] were identified by XRD. It was shown that tetragonal ZrO_2 based solid solution was single phase up to 22 mol% of $YTaO_4$ in the join ZrO_2–$YTaO_4$. Two phase field of tetragonal ZrO_2 based solid solution and scheelite was stable up to 80 mol% of $YTaO_4$. Based on experimental studies the isothermal section was constructed up to 50 mol% of Ta_2O_5. The tetragonal TaYSZ phase containing 20 mol% of $YTaO_4$ (equal fractions of $YO_{1.5}$ and $TaO_{2.5}$ of 16.6 mol%) was found to be non-transformable.[4] When the $TaO_{2.5}$ addition to 7YSZ exceeds 4 mol%, single tetragonal phase is stable but transformable to monoclinic on cooling. At higher $TaO_{2.5}$ content of 16–22 mol%, tetragonal phase becomes non-transformable.

Thermodynamic modelling: The solid solution phases (fluorite, tetragonal, cubic Y_2O_3) are described by the compound energy formalism.[24] The liquid phase is described by the two-sublattice ionic liquid model,[24] with the first sublattice filled by cations and the second one filled by anions, vacancies and neutral species. This study does not consider the metal-rich part of the system and vacancies are not included in the liquid description. The liquid is thus described by the formula $(Ta^{4+}, Y^{5+}, Zr^{4+})_P(O^{2-})_Q$, where P and Q are the number of sites on the cation and anion sublattices, respectively. The stoichiometric factors P and Q are varied with the composition in order to maintain electroneutrality. The remaining phases ($YTaO_4$ and δ-$Zr_3Y_4O_{12}$) are treated as stoichiometric compounds. The Gibbs energy of a solution phase with mixing in two sublattices (i.e. F, T, M, C, H) is expressed as

$$G = \sum_i \sum_j Y_i^s Y_j^t G_{i,j} + RT \sum_s \alpha_s \sum_i Y_i^s \ln Y_i^s + \Delta G^{ex} \quad (1)$$

where Y_i^s is the mole fraction of a constituent i in sublattice s, $G_{i,j}$ is Gibbs energy of a compound formed from species i and j, α_s is the number of sites on the sublattice s per mole of formula units of phase and ΔG^{ex} is the excess Gibbs energy of mixing expressed as

$$\Delta G^{ex} = \sum_s Y_i^s Y_j^s L_{i,j}^s + \Delta G^{tern} \quad (2)$$

where,

$$L_{i,j}^s = \sum_n (Y_i^s - Y_j^s)^n L_{i,j} \quad (3)$$

are the binary interaction parameters in the sublattice s and ΔG^{tern} is the contribution of high-order interactions. As a first approximation, the ternary and quaternary interaction parameters for the solid phases are neglected.

Thermodynamic description of the ZrO_2–Y_2O_3 system is accepted from previous work of one of the authors.[23] The thermodynamic data for the Ta_2O_5 are accepted from SGTE substance database [www.sgte.org]. Only one modification of $YTaO_4$ phase is considered in present work, because of lack of data. Heat capacity (C_P) of $YTaO_4$ phase is described as sum of C_P for oxides. Orthorhombic ZrO_2–14.3 mol.% Ta_2O_5 phase is not modelled because its stability limits are not known. Two orthorhombic phases found in the Y_2O_3–Ta_2O_5 system[17] are also not considered because of a lack of data. The fluorite and tetragonal solid solutions are presented by different formulae in the ZrO_2–Y_2O_3 and ZrO_2–Ta_2O_5 systems to keep electroneutrality. The formulae are following: $(Zr^{4+}, Y^{3+})(O^{-2}, Va)_2$ and $(Zr^{4+}, Ta^{5+}, Va)(O^{-2})_2$, respectively. Therefore, in ternary system, the formula for fluorite and tetragonal solid solutions should be presented as $(Zr^{4+}, Ta^{5+}, Y^{3+}, Va)(O^{-2}, Va)_2$, to be consistent with binary systems. The models and list of parameters used to describe phases in the ZrO_2–Ta_2O_5–Y_2O_3 system are presented in Table 1.

4. Results and discussion

4.1. Experimental results

X-ray diffraction patterns of 20TaYSZ annealed at different temperatures are shown in Fig. 1. Broad diffraction peaks indicate nanocrystalline nature of the 20TaYSZ powder annealed at 1100 °C. Nanocrystallinity is well known property of oxide powders obtained using solution chemistry routes. Diffraction peaks become sharper after treatment at 1200 °C, indicating crystallite growth with temperature. A secondary phase of m-$YTaO_4$ is clearly visible in all samples treated at temperatures below 1500 °C. $YTaO_4$ phase disappears at 1500 °C. This observation has been previously reported[4] and is also consistent with the phase diagram proposed by Kim and Tien.[5] It seems that single stable tetragonal phase forms only at 1500 °C. It is possible to see, that tetragonality of the 20TaYSZ increases with temperature (Table 2) and at 1500 °C reaches a value, which is much higher than the maximum value of 1.0203 acceptable or possible for room temperature stable phase of t-ZrO_2.[5] This means that solubility of $YTaO_4$ into ZrO_2 lattice increases with temperature

Table 1
Thermodynamic parameters for phases in the ZrO_2–Ta_2O_5–Y_2O_3 system.

Phase/temperature range	Model/parameter
IONIC_LIQUID	$(Ti^{5+},Y^{3+},Zr^{4+})(O^{2-})_2$
298.15–4000	$G(IONIC\_LIQUID,Ta^{5+}:O^{2-}) = GTA2O5 + 122000 - 57.0386932 \cdot T$
	$G(IONIC\_LIQUID,Zr^{4+}:O^{2-}) = 2 \cdot GZRO2L$
	$G(IONIC\_LIQUID,Y^{3+}:O^{2-}) = GY2O3R + 108779 - 40.509 \cdot T$
	${}^0L(IONIC\_LIQUID,Y^{3+},Zr^{4+}:O^{2-}) = 11488.4008$
	${}^1L(IONIC\_LIQUID,Y^{3+},Zr^{4+}:O^{2-}) = 1608.38521$
	$(Y^{3+}, Zr^{4+}, Ta^{5+},Va)_2\ (O^{2-})_3\ (O^{2-},Va)$
Y2O3_CUB	$G(Y2O3\_CUB,Zr^{4+}:O^{2-}:O^{2-}) = 2 \cdot GZRO2C;$
298.15–6000	$G(Y2O3\_CUB,Zr^{4+}:O^{2-}:Va) = 2 \cdot GZRO2C - GHSEROO$
	$G(Y2O3\_CUB,Y^{3+}:O^{2-}:O^{2-}) = GY2O3R + GHSEROO$
	$G(Y2O3\_CUB,Y^{3+}:O^{2-}:Va) = +GY2O3R$
	$G(Y2O3\_CUB,Ta^{5+}:O^{2-}:O^{2-}) = GTA2O5 - GHSEROO + 10.401375 \cdot T - 10000$
	$G(Y2O3\_CUB,Ta^{5+}:O^{2-}:Va) = GTA2O5 - 2\ GHSEROO - 20000 + 10.40135 \cdot T$
	$G(Y2O3\_CUB,Va:O^{2-}:Va) = 3 \cdot GHSEROO + 30000$
	$G(Y2O3\_CUB,Va:O^{2-}:O^{2-}) = 4 \cdot GHSEROO + 40000$
	${}^0L(Y2O3\_CUB,Y^{3+},Zr^{4+}:O^{2-}:O^{2-}) = -34451.2175 + 39.5035342 \cdot T$
	${}^0L(Y2O3\_CUB,Y^{3+},Zr^{4+}:O^{2-}:Va) = -34451.2175 + 39.5035342 \cdot T$
	${}^0L(Y2O3\_CUB,Zr^{4+},Ta^{5+}:O^{2-}:O^{2-}) = 120000$
	${}^0L(Y2O3\_CUB,Zr^{4+},Ta^{5+}:O^{2-}:Va) = 120000$
	${}^0L(Y2O3\_CUB,Va,Zr^{4+}:O^{2-}:O^{2-}) = 120000$
	${}^0L(Y2O3\_CUB,Va,Zr^{4+}:O^{2-}:Va) = 120000$
	${}^0L(Y2O3\_CUB,Va,Ta^{5+}:O^{2-}:O^{2-}) = 120000$
	${}^0L(Y2O3\_CUB,Va,Ta^{5+}:O^{2-}:Va) = 120000$
	${}^0L(Y2O3\_CUB,Va,Y^{3+}:O^{2-}:O^{2-}) = 120000$
	${}^0L(Y2O3\_CUB,Va,Y^{3+}:O^{2-}:Va) = 120000$
	${}^0L(Y2O3\_CUB,Ta^{5+},Y^{3+}:O^{2-}:O^{2-}) = 120000$
	${}^0L(Y2O3\_CUB,\ Ta^{5+},Y^{3+}:O^{2-}:Va) = 120000$
	${}^0L(Y2O3\_CUB,Y^{3+},Zr^{4+},Ta^{5+}:O^{2-}:O^{2-}) = 200000$
	${}^0L(Y2O3\_CUB,Y^{3+},Zr^{4+},Ta^{5+}:O^{2-}:Va) = 200000$
Y2O3_HEX	$(Y^{3+},Zr^{4+})_2\ (O^{2-})_3\ (O^{2-},Va)$
298.15–6000	$G(Y2O3\_HEX,Zr^{4+}:O^{2-}:O^{2-}) = 2 \cdot GZRO2C + 50000$
	$G(Y2O3\_HEX,Zr^{4+}:O^{2-}:Va) = 2 \cdot GZRO2C - GHSEROO + 50000$
	$G(Y2O3\_HEX,Y^{3+}:O^{2-}:O^{2-}) = GY2O3H + GHSEROO$
	$G(Y2O3\_HEX,Y^{3+}:O^{2-}:Va) = GY2O3H$
	${}^0L(Y2O3\_HEX,Y^{3+},Zr^{4+}:O^{2-}:O^{2-}) = 180000$
	${}^0L(Y2O3\_HEX,Y^{3+},Zr^{4+}:O^{2-}:Va) = 180000$
TA2O5_S	$(Ta^{5+})_2(O^{2-})_5$
298.15–6000	$G(TA2O5\_S,Ta^{5+}:O^{2-}) = GTA2O5$
TA2O5_S2	$(Ta^{5+})_2(O^{2-})_5$
298.15–6000	$G(TA2O5\_S2,Ta^{5+}:O^{2-}) = GTA2O5 + 2000 - 1.22473974 \cdot T$
ZRO2_FLU	$(Ti^{4+},Y^{3+},Zr^{4+},Va)\ (O^{2-},Va)_2$
298.15–6000	$G(ZRO2\_FLU,Zr^{4+}:O^{2-}) = GZRO2C$
	$G(ZRO2\_FLU,Zr^{4+}:Va) = GZRO2C - 2\ GHSEROO$
	$G(ZRO2\_FLU,Va:Va) = 0$
	$G(ZRO2\_FLU,Va:\ O^{2-}) = 2 \cdot GHSERO + 600000$
	$G(ZRO2\_FLU,Ta^{5+}:O^{2-}) = 0.5 \cdot GTa2O5 - 0.5\ GHSERO + 5.20069 \cdot T - 1.5E5 + 2.2E5$
	$G(ZRO2\_FLU,Ta^{5+}:Va) = 0.5 \cdot GTa2O5 - 2.5\ GHSERO + 5.20069 \cdot T - 7.5E5 + 2.2E5$
	$G(ZRO2\_FLU,Y^{3+}:O^{2-}) = 0.5 \cdot GY2O3R + 2000 + 0.5 \cdot GHSEROO + 9.3511 \cdot T$
	$G(ZRO2\_FLU,Y^{3+}:Va) = 0.5 \cdot GY2O3R + 2000 - 1.5\ GHSEROO + 9.3511 \cdot T$
	${}^0L(ZRO2\_FLU,Y^{3+},Zr^{4+}:O^{2-}) = -65401.3858 + 25.099522 \cdot T$
	${}^0L(ZRO2\_FIU,Y^{3+},Zr^{4+}:Va) = -65401.3858 + 25.099522 \cdot T$
	${}^1L(ZRO2\_FLU,Y^{3+},Zr^{4+}:O^{2-}) = 67041.1965 - 21.0271896 \cdot T$
	${}^1L(ZRO2\_FLU,Y^{3+},Zr^{4+}:Va) = 67041.1965 - 21.0271896 \cdot T$
	${}^0L(ZRO2\_FLU,Ta^{5+},Y^{3+}:O^{2-}) = 138650 - 50T$
	${}^0L(ZRO2\_FLU,Ta^{5+},Y^{3+}:Va) = 138650 - 50T$
	${}^0L(ZRO2\_FLU,Ta^{5+},Zr^{4+}:O^{2-}) = -140000$
	${}^0L(ZRO2\_FLU,Ta^{5+},Zr^{4+}:Va) = -140000$
	${}^0L(ZRO2\_FLU,Ta^{5+},Va:O^{2-}) = 50000$

Table 1 (*Continued*)

Phase/temperature range	Model/parameter
	^{0}L(ZRO2_FLU,Ta^{5+},Va:Va) = 50000
	^{0}L(ZRO2_FLU,Va,Zr^{4+}:O^{2-}) = −100000
	^{0}L(ZRO2_FLU,Va,Zr^{4+}:Va) = −100000
	^{0}L(ZRO2_FLU,Va,Y^{3+}:O^{2-}) = 50000
	^{0}L(ZRO2_FLU,Va,Y^{3+}:Va) = 50000
	^{0}L(ZRO2_FLU,Ta^{5+},Y^{3+},Zr^{4+}:O^{2-}) = 60000
	^{0}L(ZRO2_FLU,Ta^{5+},Y^{3+},Zr^{4+}:Va) = 60000
ZRO2_TETR	(Ta^{5+},Y^{3+},Zr^{4+},Va) (O^{2-},Va)$_2$
298.15–6000	G(ZRO2_TETR,Zr^{4+}:O^{2-}) = GZRO2T
	G(ZRO2_TETR,Zr^{4+}:Va) = GZRO2T − 2·GHSEROO
	G(ZRO2_TETR,Ta^{5+}:O^{2-}) = 0.5·GTa2O5 − 0.5·GHSEROO +5.20069·T − 150000–220000
	G(ZRO2_TETR,Ta^{5+}:Va) = 0.5·GTa2O5 − 2.5·GHSEROO +5.20069·T − 750000–220000
	G(ZRO2_TETR,Y^{3+}:O^{2-}) = 0.5·GY2O3R + 10000 + 0.5·GHSEROO +9.3511·T
	G(ZRO2_TETR,Y^{3+}:Va) = 0.5·GY2O3R + 10000 − 1.5·GHSEROO +9.3511·T
	G(ZRO2_TET,Va:Va) = 0
	G(ZRO2_TET,Va:O^{2-}) = 2·GHSERO + 600000
	L(ZRO2_TETR,Y^{3+},Zr^{4+}:O^{2-}) = −63233.7083 + 30·T
	L(ZRO2_TETR,Y^{3+},Zr^{4+}:Va) = −63233.7083 + 30·T
	L(ZRO2_TETR,Ta^{5+},Zr^{4+}:O^{2-}) = −160000
	L(ZRO2_TETR, Ta^{5+},Zr^{4+}:Va) = −160000
	L(ZRO2_TETR, Ta^{5+},Va:O^{2-}) = 40000
	L(ZRO2_TETR, Ta^{5+},Va:Va) = 40000
	L(ZRO2_TETR, Va,Zr^{4+}:O^{2-}) = −100000
	L(ZRO2_TETR, Va,Zr^{4+}:Va) = −100000
	L(ZRO2_TETR, Va,Y^{3+}:O^{2-}) = 50000
	L(ZRO2_TETR, Va,Y^{3+}:Va) = 50000
	L(ZRO2_TETR, Ta^{5+},Y^{3+}:O^{2-}) = 50000
	L(ZRO2_TETR, Ta^{5+},Y^{3+}:Va) = 50000
	L(ZRO2_TETR, Ta^{5+},Y^{3+},Zr^{4+}:O^{2-}) = −100000
	L(ZRO2_TETR, Ta^{5+},Y^{3+},Zr^{4+}:Va) = −100000
ZRO2_MONO	(Y^{3+},Zr^{4+}) (O^{2-},Va)$_2$
298.15–6000	G(ZRO2_MONO, Zr^{4+}:O^{2-}) = GZRO2M
	G(ZRO2_MONO, Zr^{4+}:Va) = GZRO2M − 2·GHSEROO
	G(ZRO2_MONO, Y^{3+}:O^{2-}) = 0.5·GY2O3R + 26900 + 0.5·GHSEROO +25.4·T + 9.3511·T
	G(ZRO2_MONO, Y^{3+}:Va) = 0.5·GY2O3R + 26900 − 1.5·GHSEROO +25.4·T + 9.3511·T
ZR3Y4O12(δ)	(Zr^{4+})$_3$(Y^{3+})$_4$(O^{2-})$_{12}$
298.15–6000	G(ZR3Y4O12, Zr^{4+}:Y^{3+}:O^{2-}) = 7·GZYO
YTaO4	(Y^{3+})1(Ta^{5+})(O^{2-})^4
	G(YTaO4) = 0.5·GY2O3R + 0.5·GTa2O5 − 38000 + 2.5·T
Functions	
298.15–1300	GHSERTA = −7285.88839 + 119.139649·T − 23.75926·T·ln(T) −0.0026230335·T^2 + 1.70108833·10^{-7}·T^3 − 3292.808/T
1300–2500	−22389.9623 + 243.886592·T − 41.13709·T·ln(T) + 0.00616757·T^2 −6.55135667 × 10^{-7}·T^3 + 2429586/T
2500–3290	+229382.916 − 722.597463·T + 78.52448·T·ln(T)−0.017983375·T^2 +1.95033·10 − 7·T^3 − 93813650/T
3290–6000	−42882.7013 + 269.225623·T − 41.84·T·ln(T)
298.15–1000	GHSEROO = −3480.87 − 25.503038·T − 11.1355·T·ln(T) −0.005098875·T^2 + 6.61845833·10^{-7}·T^3 − 38365/T
1000–3300	−6568.763 + 12.659879·T − 16.8138·T·ln(T) − 5.957975 × 10^{-4}·T^2 +6.781E − 09·T^3 + 262905/T
3300–6000	−13986.728 + 31.259624·T − 18.9536·T·ln(T) − 4.25243 × 10^{-4}·T^2 +1.0721 × 10^{-8}·T^3 + 4383200/T
298.15–1000	GHSERYY = −8011.09379 + 128.572856·T − 25.6656992·T·ln(T) −0.00175716414·T^2 − 4.17561786·10 − 7·T^3 + 26911.509/T

Table 1 (*Continued*)

Phase/temperature range	Model/parameter
1000–1795.15	$-7179.74574 + 114.497104 \cdot T - 23.4941827 \cdot T \cdot \ln(T) - 0.0038211802 \cdot T^2 - 8.2534534 \times 10^{-8} \cdot T^3$
1795.15–3700	$-67480.7761 + 382.124727 \cdot T - 56.9527111 \cdot T \cdot \ln(T) + 0.00231774379 \cdot T^2 - 7.22513088 \cdot 10^{-8} \cdot T^3 + 18077162.6/T$
298.15–2128	$GHSERZR = -7827.595 - 125.64905 \cdot T - 24.1618 \cdot T \cdot \ln(T) - 0.00437791 \cdot T^2 + 34971/T$
2128–6000	$-26085.921 + 2622.724183 \cdot T - 42.144 \cdot T \cdot \ln(T) - 1.342895 \cdot 10^{-31} \cdot T^{-9}$
298.15–1633	$GTa2O5 = -2103104.07 + 893.195926 \cdot T - 151.255 \cdot T \cdot \ln(T) - 0.015530075 \cdot T^2 - 1.40927433 \times 10^{-10} \cdot T^3 + 1136975/T$
1633–2150	$-2156227.05 + 1335.39795 \cdot T - 210 \cdot T \cdot \ln(T) + 1.6681945 \times 10^{-14} \cdot T^2 - 1.104863 \times 10^{-18} \cdot T^3 + 1.3622705 \times 10^{-5}/T$
2150–6000	$-2177727.05 + 1422.13018 \cdot T - 220 \cdot T \cdot \ln(T) + 1.7185345 \times 10^{-16} \cdot T^2 - 5.45587 \times 10^{-21} \cdot T^3 + 4.627957 \times 10^{-7}/T$
298.15–6000	$GZRO2M = -1126163.54 + 424.890806 \cdot T - 69.3875137 \cdot T \cdot \ln(T) - 0.00375880141 \cdot T^2 + 683000/T$
298.15–6000	$GZRO2T = GZRO2M + 5468 - 4.0 \cdot T$
298.15–6000	$GZRO2C = GZRO2 + 10336 - 4.0 \cdot T$
298.15–6000	$GZRO2L = GZRO2 + 87027 - 29.17432 \cdot T$
298.15–6000	$GY2O3R = -1976462 + 731.6512 \cdot T - 121.881 \cdot T \cdot \ln(T) - 0.00506 \cdot T^2 + 1090000/T - 13000000/T^2$
298.15–6000	$GY2O3H = GY2O3R + 25100 - 9.654 \cdot T$
298.15–6000	$GZYO = 0.4286 \cdot GZRO2C + 0.2857 \cdot GY2O3R - 14550.3912 - 0.520412688 \cdot T$
298.15–6000	

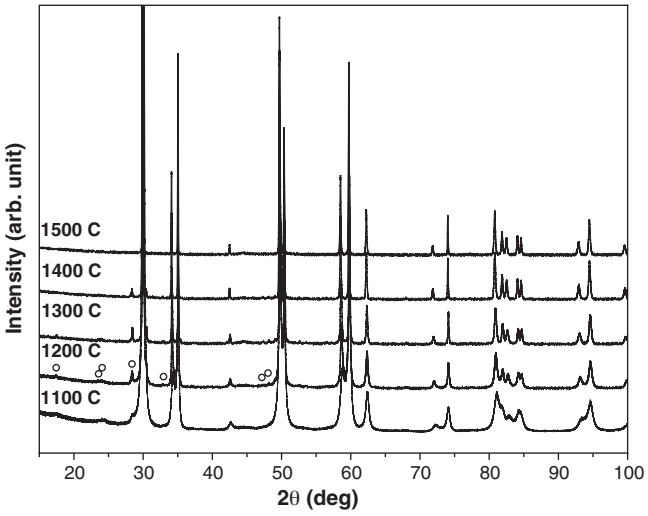

Fig. 1. Room temperature X-ray powder diffraction patterns of 16TaYSZ heat treated for 4 h at different temperatures (◯: $YTaO_4$).

Table 2
Variation of tetragonality of 20TaYSZ phase with temperature *T*.

T, °C	Tetragonality[a]
1100	1.0212
1200	1.0248
1300	1.0255
1400	1.0258
1500	1.0262

[a] Tetragonality was calculated as $c/a\sqrt{2}$.

and tetragonality increases with the increase of $YTaO_4$ content. The 20TaYSZ sample corresponds to a system where ZrO_2 is doped with 20 mol% $YTaO_4$. The *c*/*a* value of this composition at 1500 °C is calculated to be 1.0262, what agrees well with the reported value elsewhere.[25] 20TaYSZ pretreated at 1500 °C remains stable when treated for 600 h at 1250 °C. Fig. 2 shows the XRD patterns of pretreated (at 1500 °C) 20TaYSZ sample which was later treated at 1250 °C for 4 h and 600 h. No phase change observed upon long term annealing at 1250 °C. However, some weak reflections at $2\Theta = 28.4$ and 58.8 can be seen. Though it is difficult to analyse these weak overlapping peaks but it can be m-$YTaO_4$ and/or orthorhombic Y_3TaO_7 and/or orthorhom-

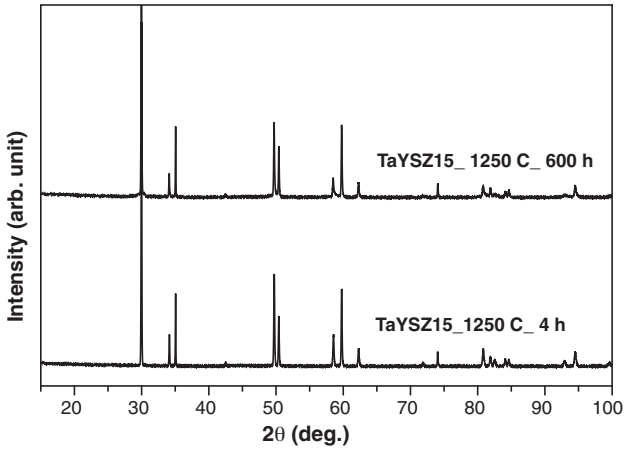

Fig. 2. Room temperature X-ray powder diffraction pattern of TaYSZ15 treated at 1250 °C for 4 h and 600 h.

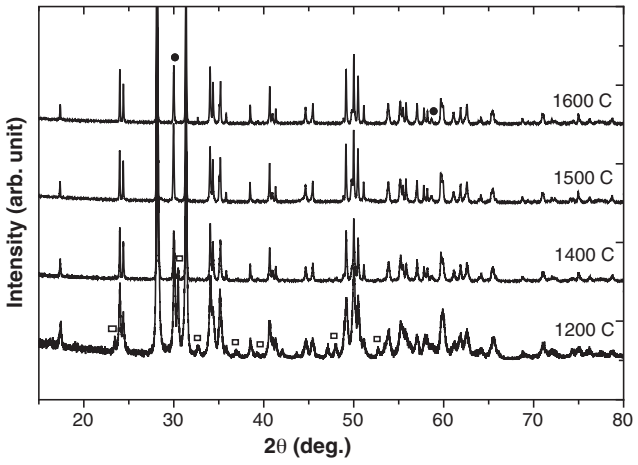

Fig. 3. Room temperature X-ray powder diffraction patterns of 10TaYSZ heat treated for 4 h at different temperatures (●: t-TaYSZ, ■:m-$YTaO_4$).

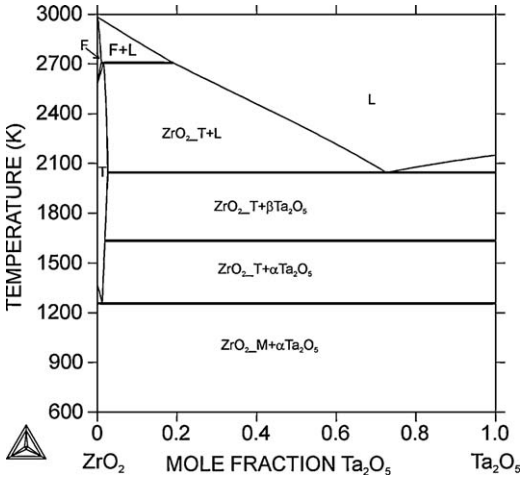

Fig. 4. Calculated isothermal section of the ZrO_2–Ta_2O_5 system.

bic $Y_{2.8}Ta_{1.17}O_{2.8}$ as found by search and match from ICSD database (www.icsdweb.fiz-karlsruhe.de).

Another composition prepared in this work was $Y_{0.1}Ta_{0.1}Zr_{0.8}O_2$ which corresponds to 11 mol% $YTaO_4$ doped ZrO_2. According to previous works[5,25] this composition should correspond to t-ZrO_2 and m-ZrO_2 solid solutions at room temperature after being treated at 1500 °C. X-ray diffraction patterns of 11TaYSZ sample treated at different temperatures (Fig. 3) show that at all temperatures m-ZrO_2 ss ('ss' stands for solid solution) is the major phase with t-TaYSZ and m-$YTaO_4$ as the minor phases. Peaks corresponding to $YTaO_4$ phase can be seen up to 1400 °C. Above 1400 °C the $YTaO_4$ phase disappears.

Dissolution of $YTaO_4$ phase in the ZrO_2 lattice at and above 1400 °C in 20TaYSZ and 11TaYSZ systems is related to the transformation of monoclinic $YTaO_4$ into tetragonal $YTaO_4$ at that temperature. The resulted t-$YTaO_4$ has scheelite-like structure,[26] which enhances solubility of $YTaO_4$ in t-ZrO_2 above 1400 °C.

4.2. Preliminary thermodynamic description

The thermodynamic parameters of fluorite and tetragonal phases were assessed in the ZrO_2–Ta_2O_5 system to reproduce small solubility of Ta_2O_5 (∼2 mol%) in these phases. The parameters of liquid phase were not optimised because phase diagram at high temperatures is not known. The calculated isothermal cross-section ZrO_2–Ta_2O_5 system is presented in Fig. 4.

The Gibbs energy of the $YTaO_4$ phase and the Gibbs energies and mixing parameters of Y_2O_3_C (cubic) phase were estimated to reproduce experimental solubility of Ta_2O_5 in the cubic Y_2O_3 phase and stability of the $YTaO_4$ phase up to high temperatures. Additionally, parameters of fluorite phase were estimated to comply with the stability of fluorite phase (Y_3TaO_7) at high temperatures. Calculated composition of the fluorite phase shifted in Y_2O_3 rich region. Probably, taking into account orthorhombic phases will improve the results. The parameters of liquid were not optimised due to the large uncertainty of experimental data at high temperatures. The mixing parameters of tetragonal phase were estimated to be close to the fluorite phase but with slightly more positive values assigned to them to avoid appearance of tetragonal phase in the Y_2O_3–Ta_2O_5 system. Calculated phase diagram of the Y_2O_3–Ta_2O_5 system is presented in Fig. 5.

The binary descriptions were combined in ternary. The ternary mixing parameter of tetragonal phase and the Gibbs energy of $YTaO_4$ were adjusted to agree with the experimentally indicated tie lines in ternary system and maximal solubility of Ta_2O_5 and Y_2O_3 in tetragonal phase. The calculated isothermal section of the ZrO_2–Ta_2O_5–Y_2O_3 system at 1500 °C is presented in Fig. 6a. The homogeneity range of tetragonal phase is narrow and extended in the direction of $YTaO_4$. Maximal content of Ta_2O_5 in fluorite structure reaches 4.5 mol %. The calculated phase diagram is in a reasonable agreement with experimental results obtained earlier.[5] The isothermal section calculated at 1200 °C is presented in Fig. 6b. It is quite similar to phase diagram at 1500 °C. The calculated composition of tetragonal phase in equilibrium with $YTaO_4$ and Ta_2O_5 is practically the same for both temperatures. The contrast to isothermal section at 1500 °C are the δ-phase which is stable at 1200 °C, decreased maximal content of Ta_2O_5 in fluorite structure to 2.7 mol % and the com-

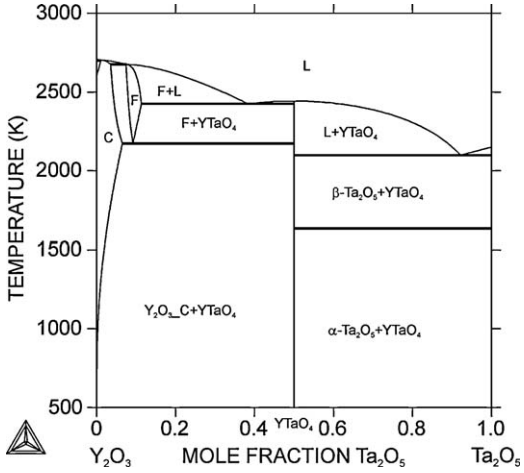

Fig. 5. Calculated phase diagram of the Y_2O_3–Ta_2O_5 system.

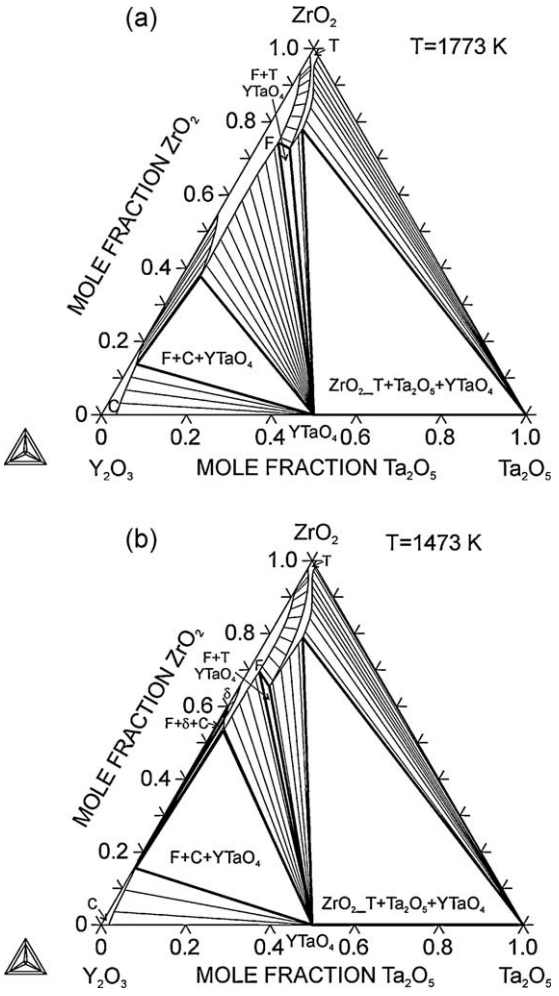

Fig. 6. Calculated isothermal section of the ZrO_2–Ta_2O_5–Y_2O_3 system at 1500 °C (a) and at 1200 °C (b).

position of tetragonal phase in equilibrium with fluorite structure and $YTaO_4$ changes with lower ZrO_2 and higher Y_2O_3 content compared to that at 1500 °C. It should be mentioned that temperature dependence of ternary mixing parameter was not optimised due to absence of reliable data on temperature dependence of maximal solubility of $YTaO_4$ in tetragonal phase. It is important to underline that the obtained thermodynamic description is preliminary and further improvement is required such as taking into account monoclinic phase of $YTaO_4$ and orthorhombic phase $Ta_2Zr_6O_{17}$. Measurement of thermodynamic properties for $YTaO_4$ and orthorhombic phase $Ta_2Zr_6O_{17}$ and including them into thermodynamic database should provide better fit of experimental data. On the other hand, the experimental studies at temperatures lower than 1500 °C indicate that equilibrium is not achieved and thus thermodynamic calculations will allow us to estimate equilibrium phase relation at lower temperatures.

5. Conclusion

The preliminary thermodynamic description of the ZrO_2–Ta_2O_5–Y_2O_3 system is derived showing phase relations at 1500 °C and at 1200 °C. Ternary diagram obtained here is in good agreement with previously derived one at 1500 °C. The ternary phase diagram at 1200 °C has been derived here for the first time. The stability region of tetragonal solid solution (T) is almost unaffected by variation of temperature. This is also complimented from our experimental results. It has been shown that once $YTaO_4$ gets soluble in t-ZrO_2 at 1500 °C, this phase does not appear when annealed at low temperature for long duration. However, some weak reflections are about to appear upon long term annealing. Hence, experimental studies of thermodynamic properties of the $YTaO_4$ are highly necessary to get more exact thermodynamic parameters in the binary and ternary system. Further studies of the stability of orthorhombic phase in the ZrO_2–Ta_2O_5 system and its thermodynamic properties are in due course. Information about phase composition of tetragonal and fluorite structure in ternary system at different temperatures is needed to make full assessment of thermodynamic parameters of these phases.

Acknowledgements

Authors are indebted to Innovation Promotion Agency (CTI) of Swiss Federal Office for Professional Education and Technology (Project 8974.1 PFIW-IW) for financial support.

References

1. Levi CG. Emerging materials and processes for thermal barrier coatings. *Curr Opin Solid State Mater Sci* 2004;**8**:77–91.
2. Jones RL, Mess D. Improved tetragonal phase stability at 1400 °C with scandia, yttria-stabilized zirconia. *Surf Coat Technol* 1996;**86–87**:94–101.
3. Miller RA, Smialek JL, Garlick RG. *Science and technology of zirconia*. Columbus, OH: Am. Ceram. Soc., Inc.; 1981. p. 241.
4. Pitek FM, Levi CG. Opportunities for TBCs in the ZrO_2–$YO_{1.5}$–$TaO_{2.5}$ system. *Surf Coat Technol* 2007;**201**:6044–50.
5. Kim DJ, Tien TY. Phase stability and physical properties of cubic and tetragonal ZrO_2 in the system ZrO_2–Y_2O_3–Ta_2O_5. *J Am Ceram Soc* 1991;**74**:3061–5.
6. Li P, Chen IW, Penner-Hahn JE. Effect of dopands on zirconia stabilization—An X-ray absorption study. III. Charge-compensating dopants. *J Am Ceram Soc* 1994;**77**:1289–95.
7. Kim DJ. Effect of Ta_2O_5, Nb_2O_5 and HfO_2 alloying on the transformability of Y_2O_3-stabilised tetragonal ZrO_2. *J Am Ceram Soc* 1990;**73**:115–20.
8. Ho SM. On the structural chemistry of zirconium oxide. *Mater Sci Eng* 1982;**54**:23–9.
9. Raghavan S, Wang H, Porter WD, Dinwiddie RB, Vassen R, Stoever D, et al. Ta_2O_5/Nb_2O_5 and Y_2O_3 co-doped zirconias for thermal barrier coatings. *J Am Ceram Soc* 2004;**87**:431–7.
10. TCC. *Thermo-Calc software*. Stockholm, Sweden: Stockholm Technology Park; 2006.
11. Lukas H, Fries S, Sundman B. *Computational thermodynamics. The CALPHAD method*. Cambridge University Press; 2007.
12. Roth RS, Waring JL. Effect of oxide additions on the polymorphism of tantalum pentoxide III. Stabilization of the low temperature structure type. *J Res Natl Bur Stand A: Phys Chem* 1970;**74A, 4**:485–93.
13. King, B.W., Schultz, J., Durbin, E.A. and Duckworth, W.H., Properties of Tantala Systems. U.S.A.E.C., Report No. BMI-1106, 1956, 1–40.
14. Zheng C, West AR. Compound and solid solution formation phase equilibria and electrical properties in the ceramic system ZrO_2–La_2O_3–Ta_2O_5. *J Mater Chem* 1991;**1, 2**:163–7.
15. Bondar IA, Kalinin AI, Koroleva LN. Physico-chemical investigation of the system Y_2O_3–Ta_2O_5 and the synthesis of single crystals of a number of tantalates. *Izv Akad Nauk SSSR, Inorg Mater (Engl Transl)* 1972;**8, 10**:1649–50.

16. Vasil'ev VS, Pinaeva MM, Shkirman SF. *Russ J Inorg Chem (Engl Transl)* 1979;**24, 4**:578–82.
17. Yokogawa Y, Yoshimura M. High temperature phase relations in the system Y_2O_3–Ta_2O_5. *J Am Ceram Soc* 1991;**74, 9**:2077–81.
18. Yokogawa Y, Yoshimura M. Formation and stability regions of the high-temperature fluorite-related phases in the R_2O_3–Ta_2O_5 system (R = La, Nd, Sm, Ho, Er and Yb). *J Am Ceram Soc* 1997;**80, 8**: 1965–74.
19. Yashima M, Tsuji T. Crystal structure, disorder, and diffusion path of oxygen ion conductors $Y_{1-x}Ta_xO_{1.5+x}$ ($x = 0.215$ and 0.30). *Chem Mater* 2007;**19, 14**:3539–44.
20. Kim S, Yashima M, Kakihana M, Yoshimura M. Electrical properties of defect-fluorite phase in the system R_2O_3–Ta_2O_5 (R = Gd, Y, Er and Yb). *J Alloys Compd* 1993;**192**:72–4.
21. Fabrichnaya O, Aldinger F. Assessment of thermodynamic parameters in the system ZrO_2–Y_2O_3–Al_2O_3. *Z Metallkd* 2004;**95**:27–39.
22. Fabrichnaya O, Wang C, Zinkevich M, Levi CG, Aldinger F. Phase equilibria and thermodynamic properties of the ZrO_2–$GdO_{1.5}$–$YO_{1.5}$ system. *J Phase Equilibr Diffus* 2005;**26**:591–604.
23. Fabrichnaya O, Zinkevich M, Aldinger F. Thermodynamic modelling in the ZrO_2–La_2O_3–Y_2O_3–Al_2O_3 system. *Int J Mater Res* 2007;**98, 9**:838–46.
24. Hillert M. The compound energy formalism. *J Alloys Compd* 2001;**320, 2**:161–76.
25. Kim DJ, Hubbard CR. X-ray powder diffraction data for tetragonal zirconia solid solutions in system ZrO_2–$YTaO_4$. *Powder Diffr* 1992;**7**:174–5.
26. Mather SA, Davies PK. Nonequilibrium phase formation in oxides prepared at low temperature: fergusonite-related phases. *J Am Ceram Soc* 1995;**78**:2737–45.